Enhancing Oil Removal from Water using Ferric Oxide Nanoparticles Doped Carbon Nanotubes Adsorbents

Ahmad Kayvani Fard, Tarik Rhadfi, Gordon Mckay, Mohammed Al-marri, Ahmed Abdala, Nidal Hilal, Muataz A. Hussien

PII: S1385-8947(16)30141-3
DOI: http://dx.doi.org/10.1016/j.cej.2016.02.040
Reference: CEJ 14773

To appear in: *Chemical Engineering Journal*

Received Date: 19 December 2015
Revised Date: 10 February 2016
Accepted Date: 12 February 2016

Please cite this article as: A.K. Fard, T. Rhadfi, G. Mckay, M. Al-marri, A. Abdala, N. Hilal, M.A. Hussien, Enhancing Oil Removal from Water using Ferric Oxide Nanoparticles Doped Carbon Nanotubes Adsorbents, *Chemical Engineering Journal* (2016), doi: http://dx.doi.org/10.1016/j.cej.2016.02.040

Enhancing Oil Removal from Water using Ferric Oxide Nanoparticles Doped Carbon Nanotubes Adsorbents

Ahmad Kayvani Fard[a,b], Tarik Rhadfi[a], Gordon Mckay[b], Mohammed Al-marri[d], Ahmed Abdala[a,b], Nidal Hilal[a, c] Muataz A. Hussien[a,b1]

[a]Qatar Environment and Energy Research Institute, Hamad Bin Khalifa University, Qatar Foundation, PO Box 5825, Doha, Qatar.

[b]College of Science and Engineering, Hamad Bin Khalifa University, Qatar Foundation, PO Box 5825, Doha, Qatar.

[c]Centre for Water Advanced Technologies and Environmental Research, (CWATER) College of Engineering, Swansea University, Swansea SA2 8PP, United Kingdom.

[d]Gas Processing Center (GPC), Qatar University, Doha, Qatar

Abstract

Oil contaminated water is one of the challenges in water resources management. It is crucial to remove the oil droplets from water in order to meet the discharge regulations set by the environmental authorities. Carbon nanotubes (CNTs) have generated a lot of attention as a new type of adsorbent due to their exceptionally high adsorption capacity for oil-water separation. The high hydrophobicity of CNTs makes them good candidates to enhance the de-oiling process from wastewater. In this study, we have reported the synthesis and evaluation of novel iron-oxide/CNTs nanocomposites for oil-water separation. The CNTs were doped with different

[1] Corresponding author. E-mail address: mhussien@qf.org.qa (M. Ali Atieh).

loadings of iron oxide nanoparticles using a wet impregnation technique. The synthesized nanocomposite nanomaterials were characterized using field emission scanning electron microscopy (FE-SEM), high resolution transmission electron microscopy (TEM), Brunauer, Emmett and Teller (BET) technique, X-ray Diffraction (XRD), and thermogravimetric analysis (TGA). The effect of adsorption parameters, including, adsorbent dosage, contact time, and agitation speed on the oil removal efficiency were optimized using batch experiments. The sorption capacities of doped CNTs were found to be greater than 7 g/g for gasoline oil. The doped CNTs reached maximum sorption capacity after only 15 minutes providing one of the fastest minimum contact times reported of all oil sorbent materials. The loading of Fe_2O_3 nanoparticles on the negative surface of CNT decreases the negative sign and magnitude of the zeta potential by overcoming the repulsive effects of the electrical double layers to allow the finely sized oil droplets to form larger droplets through coalescence. Therefore increasing percentage of the Fe_2O_3 on the surface of CNT increased the removal of the emulsified oil from the water.

1. Introduction

The rapid economic growth in the world has increased the demand for oil, since oil is one of the major sources of energy and raw materials for so many products such as polymers, petrochemicals, fuels and many other products. The use of oil and oil-based products has increased globally to approximately 100 million tonnes per year. Reports [1] indicate that, from 2000 to 2011 more than 224,000 tonnes of oil were released into the seas and oceans globally, due to spillages from oil tankers. This does not include oil discharges from oil extraction platforms due to spillage [1]. Moreover, another source of oil contamination is the produced water during the oil exploration stage. The global production rate of produced water is estimated

to be around 250 million barrels per day for the extraction of 80 million barrels per day of oil. As a result, 3 barrels of contaminated produced water are produced per each barrel of oil extracted [2]. Due to large-scale extraction of oil that generates large amounts of produced water, oil pollution from this source has become one of the major threats to the environment and has become a global concern due to its toxicity and economic value.

When oil mixes with the water, it forms an oil- water emulsion or floating film that should be removed before it is discharged into the environment. Due to the large generation of produced water and also oil contaminated water by the oil industries, many countries are focusing efforts to find cost-effective and efficient treatment technologies to remove emulsified oil particles from water as a way to augment their limited fresh water resources. Such water, if treated to meet the environmental limits and regulations, can be used as aquifer recharge, irrigation, livestock or wildlife watering and habitats, and industrial applications (e.g. vehicle washing, power plant cooling water, and fire control) [3]. The United States Environmental Protection Agency (USEPA) limits the daily maximum limit of oil and grease in water as 42 mg/L and the monthly average limit is 29 mg/L [4].

Different techniques are reported in the literature for treating oil-contaminated water and some examples of the techniques are: reverse osmosis, filtration (ultra and micro), various flotation methods (dissolved air, column flotation, electro and induced air), adsorption, gravity separation, activated sludge treatment, membrane bioreactors, biological treatment, chemical coagulation, electro-coagulation and coalescence [5].

Adsorption/sorption is believed to be one of the optimal processes for the removal of oil from water due to its low operational and capital cost as well as its high removal efficiency. Different

materials have been reported in literature as oil de-emulsifiers for oil-water treatment such as natural sorbents, organic polymers (synthetic) and mineral materials (inorganic) [6].

The selection of adsorbents and development of new functional materials that can achieve de-oiling from water is an important practice and depends on many factors, such as the availability of the material, cost of material, and material safety. Materials with high carbon or oxygen contents have also been identified for high oil capacity uptake from water. Other physical factors such as surface area, surface charge density, and oil uptake capacity, thermal and mechanical stability are other important factors for choosing an appropriate adsorbent. Nevertheless, only a limited numbers of materials meet all the practical demands for oil selectivity, sorption capacity, sorption rate, and recyclability. These parameters, which are mainly controlled by the structures of the adsorbents that exhibit super-hydrophobicity, high porosity, suitable pore sizes, and reversible deformation under a high level of strain, must be studied and considered [7-10]. Until now, the synthesis of sorbents with superior oil sorption performance has remained a great challenge.

Super-hydrophobicity is a function which is mainly found on hydrophobic surfaces with enhanced surface roughness because of the minimization of contact areas between the surface and water by trapped air [11, 12]. Therefore, multi-walled carbon nanotubes (MWCNTs; we refer to them in this paper as CNTs for the sake of simplicity), have been widely used for the synthesis of super-hydrophobic surfaces because of their large aspect ratio, chemical inertness, and hydrophobicity [13, 14].

Carbon nanotubes (CNTs) as a new type of carbon materials are widely used in many fields. Since their discovery in 1991, they have attracted a lot of interest due to their chemical,

mechanical, and thermal stability [15, 16]. Oil-water separation using CNTs as an adsorbent agent has been reported by a limited number of researchers and considered to be a new field for development.

Gui et al. [17, 18] used magnetic carbon nanotube (me-CNT) sponges as a new sorbent material for spilled oil recovery. The magnetic sponges showed mass sorption capacities for diesel oil of up to 56 g/g, while Zhao et al. [19] prepared sponge-like exfoliated vermiculite (EV)/carbon nanotube (CNT) hybrids with different CNT percentages by introducing aligned CNT arrays into natural vermiculite layers for oil adsorption. The highest adsorption capacity of the EV/CNT hybrids was 26.7 g/g for diesel oil with EV/CNT hybrids having 91%. Table (1) summarizes some previous studies on the oil spills clean-up using different types of CNT. In the studies listed in Table 1, oil-water separation occurs as oil spill clean-up where only free oil is adsorbed by the adsorbent and emulsified oil has not been investigated.

In this study we reported the effects of undoped and doped CNTs with different weight loadings of Fe_2O_3 nanoparticles adsorbents on the separation of emulsified gasoline oil droplets from water. The oil and water is mixed very well to form a very uniform emulsion before adsorption process. It worth mentioning, the adsorption process removes both mixed and free oil from water in comparison to the oil spill clean-up which only adsorbs the oil on the surface. The undoped and doped CNTs were characterized using field emission scanning electron microscopy (FE-SEM), high transmission electron microscopy (HR-TEM), thermogravimetric analysis (TGA), X-ray diffractometer (XRD), the Brunauer, Emmett and Teller (*BET*) nitrogen adsorption technique, and Zeta potential. The effect of different parameters such as adsorbent dosage, contact time, and oil concentration were investigated and optimum parameters for maximum removal of oil have been investigated. The adsorption experimental equilibrium data were

correlated by the Langmuir and Freundlich isotherms, while the sorption energy was calculated using the Tempkin model. The kinetic data were analyzed using three kinetic models.

2. Materials and methods

2.1.Material

The CNTs used in this study were purchased from the Chengdu Organic Chemicals Co Ltd. (China) with purity>95%, lengths of 1–10 μm, outer diameters of 10–20 nm and nitrogen BET surface area of 156 m^2/ g. Ethanol liquid (98%, purity) as solvent and ferric nitrate ($Fe(NO_3)_3.9H_2O$ (99 % purity), as a precursor of the iron nanoparticles, were obtained from Sigma-Aldrich Co Ltd. Gasoline liquid as an oil source was purchased from local petrol distribution company, Woqod, Doha, Qatar with an octane number of 97. All the chemicals were used without further purification.

2.2. Preparation of modified α-Fe_2O_3/CNT

The surface modification of CNTs by iron oxide nanoparticles was carried using the wet impregnation method. A fixed amount of ferric nitrate was dissolved in 500 ml of liquid ethanol containing a fixed amount of CNTs. Different loadings of iron oxide nanoparticles (1, 10, 30 and 50 wt%) were prepared by changing the concentration of ferric nitrate in aqueous ethanol solutions. The solutions were sonicated for 45 minutes using a prop sonicator to disaggregate the agglomeration of CNTs and disperse them homogeneously into the solutions. The aqueous solution was evaporated at 70 °C in a convection oven. The residue was calcinated at 350 °C for 4 hours in an oven in the presence of air to prepare the iron oxide nanoparticles from iron nitrate (Figure 1).

2.3.CNT characterization

Powder X-ray diffraction (XRD) patterns were recorded by using a Rigaku MiniFlex-600 and the X-Ray diffractometer with Cu Kα radiation λ = 1.54Å at a rate of 0.4 % over Bragg angles ranging from 10–90 degrees. The operating voltage and current were maintained at 40 kV and 15 mA, respectively. The morphologies of the samples were analyzed with TESCAN MIRA 3 FEG-SEM, field emission scanning electron microscope using an acceleration voltage of 20 kV. The elemental analysis (Fe, C, and O) was performed with EDX analysis. The surface areas of the undoped and doped CNTs were measured by N_2 adsorption at 77 K using BET surface area analyzer Micromeritics ASAP 2020. In order to determine the amount of Fe_2O_3 present on the CNT surface, thermogravimetric analyses were performed with a TGA analyzer (Q50 K.U. Leuven SDT, Q600) at a heating rate of 10 °C/min in air. The surface charge density of the nanoparticles was measured using Zetasizer (Nano ZS 90, Malvern Instruments Ltd., Malvern, UK) equipped with a 4.0 mW internal laser, which works on the principle of dynamic light scattering (DLS). The measurements were performed at room temperature (25 °C), with a scattering angle of 90°. The initial and final concentrations of the emulsified oil in water were measured using a combustion type TOC analyzer (Shimadzu, model TOC-L; detection range of 4 µg/L to 30,000 mg/L).

2.4. Batch experiments

The effects of adsorption parameters on the adsorption capacity of oil removal from water by undoped and doped CNTs with different loading of Fe_2O_3 nanoparticles were investigated using batch mode experiments. In these experiments, the effects of adsorbent dosage, initial oil

concentration, and contact time on the percentage removal and adsorption capacity of emulsified oil from water were studied. The adsorption capacity (Q) and removal efficiency (RE) were calculated as follows:

$$Q = \frac{(C_i - C_f) \times V}{W_g} \qquad (1)$$

$$RE\ (\%) = \frac{(C_i - C_f)}{C_i} \times 100 \qquad (2)$$

Where C_i (mg/L) is the initial concentration of emulsified oil in the water, C_f (mg/L) is the final concentration of the remaining oil in the water, V (L) is the volume of the water, and W_g is the mass of CNTs.

All the batch experiments were performed by adding 20 mL of aqueous solution containing specific concentrations of oil to 20 mg of undoped and doped CNTs. The experiments were performed at room temperature. While the effect of the oil concentrations on the adsorption capacity was examined by varying the initial oil concentration from 425 to 7460 mg/L. The equilibrium studies were carried out for 120 min to determine the equilibrium contact time and uptake capacity. To find the optimum amount of adsorbent dosages for maximum removal of emulsified oil from water, different weights of undoped and doped CNTs were varied from 5 to 35 mg. All the samples were agitated using a mechanical shaker at 400 rpm.

2.5. Adsorption kinetic study

The aqueous solutions (20 ml) with 20mg of undoped and doped CNTs were agitated at 400 rpm using a mechanical shaker at 27 °C. The samples (1.2 ml) were taken from the solution at each preset time intervals and the final concentrations of oil were analyzed using a TOC analyzer.

In order to find the maximum oil uptake by CNTs and to interpret the experimental data, three kinetic models, pseudo-first-order, pseudo-second-order, and intraparticle diffusion models were used in this study. A linear fitting procedure using Origin software was also used to analyze the experimental uptake rate date.

The Lagergren pseudo-first-order model proposes that the rate of sorption is proportional to the number of sites unoccupied by the adsorbate [24]. The pseudo-first-order equation can be written in linearized form as follows:

$$\ln(Q_e - Q_t) = \ln Q_e - k_1 t \qquad (3)$$

Where Q_t is the sorption capacity (mg/g) at any preset time interval (t) and k_1 is the pseudo first-order rate constant (min^{-1}). A graph of $\ln(Q_e\text{-}Q_t)$ versus time is plotted and the constant is found. Additionally, the adsorption data were analyzed using the pseudo-second-order kinetic model [25]. The pseudo-second-order kinetic model can be written in linearized form as follows:

$$\frac{t}{Q_t} = \frac{1}{k_2 Q_e^2} + \frac{t}{Q_e} \qquad (4)$$

Where k_2 is the second-order rate constant (g/mg.min). By plotting t/Q_t versus time, straight lines were obtained and the constants, k_2 and Q_e, were found.

In order to gain insight into the mechanisms and rate controlling steps affecting the kinetics of adsorption, the kinetic experimental results were fitted to the Weber–Morris intraparticle diffusion (IPD) model which is commonly expressed using the following equation [26]:

$$Q_t = k_i t^{\frac{1}{2}} + C \qquad (5)$$

Where k_i is the intraparticle diffusion rate constant (mg/g.min) and C (mg/g) is the intercept.

The larger the intercept, the greater the contribution of the surface sorption in the rate-controlling step will be. If the graph of Q_t vs $t^{1/2}$ is linear and passes through the origin, intraparticle diffusion is the sole rate-limiting step for the adsorption process.

2.6. Adsorption Isotherm

The maximum adsorption capacity and the sorption energy of oil on CNTs were analyzed using Freundlich, Langmuir, and Temkin isotherm models. The Freundlich isotherm can be expressed by the equation:

$$Q_e = K_F C_e^{\frac{1}{n}} \qquad (6)$$

Where C_e is the adsorbate concentration at equilibrium (mg/L), Q_e is the adsorption capacity at equilibrium, and n and K_F are Freundlich empirical constants that indicate the sorption intensity and the sorption capacity of the adsorbent, respectively. The above equation can be linearized and expressed as:

$$\ln Q_e = \ln K_F + \frac{1}{n} \ln C_e \qquad (7)$$

The Freundlich model does not consider the maximum sorption saturation, as it assumes a heterogeneous adsorbent surface and an energy distribution for the different sites.

On the other hand, the Langmuir isotherm model assumes that the adsorption takes place at defined homogeneous sites on the surface of the adsorbent. The Langmuir isotherm is expressed by the equation:

$$Q_e = \frac{X_m K C_e}{(1+KC_e)} \qquad (8)$$

Where C_e is the equilibrium concentration of adsorbate in aqueous solution (mg/g), Q_e is the adsorption density at the equilibrium solution concentration C_e, K is the Langmuir constant, and X_m is the maximum oil adsorption capacity (mg/g).

The Langmuir isotherm model assumes that when adsorption takes place at defined homogeneous sites on the surface of the adsorbent, suggesting that once an oil molecule occupies a site, no further adsorption can take place at that occupied site. The above equation can be rearranged to give the linearized equation expressed as:

$$\frac{C_e}{Q_e} = \frac{1}{X_m K} + \frac{C_e}{X_m} \qquad (9)$$

The Langmuir constants K and X_m (which are related to the constant free energy of sorption) can be determined by representing linear plot of C_e/Q_e vs. C_e from the intercept and slope of the plot.

2.7. Sorption Energy

The Temkin isotherm assumes that, the sorption energy during the sorption process decreases linearly with increasing sorption site saturation rather than decreasing exponentially, as implied by the Freundlich isotherm. The Temkin isotherm is given as [27]:

$$Q_e = \frac{RT \ln(AC_e)}{b} \qquad (10)$$

The Temkin isotherm can be linearized as follow:

$$Q_e = B \ln A + B \ln C_e \qquad (11)$$

Where B = RT/b, b is the Temkin constant related to the sorption energy, A is the equilibrium binding constant (L/mg) and B is constant related to the heat of sorption. The linearized isotherm coefficients were estimated using graphical methods by plotting Q_e vs ln C_e and are reported throughout the paper.

3. Results and discussion

3.1. Characterization of CNT and Fe-doped CNT

The undoped and doped CNTs were characterized using field-scanning electron microscopy (FE-SEM), high resolution Transmission Electron Microscopy (HR-TEM), Thermogravimetry (TGA) techniques, XRD, BET surface area and Zeta potential.

The surface morphologies of the undoped and doped CNTs adsorbents were observed using FE-SEM. Figure 2 shows the SEM images of undoped and doped CNTs with 1 and 10, wt% of Fe_2O_3 nanoparticles. The diameter of the CNTs varies from 20–40 nm with an average diameter of 24 nm. It can be observed that, there are no changes on the surfaces of doped CNTs after doping. They are agglomerating and untangled similar to a cotton like structure.

High Resolution Transmission Electron Microscopy (HR-TEM) was performed to characterize the structures, sizes and the purity of undoped and doped carbon nanotubes with iron oxide nanoparticles. The TEM image of the unmodified nanotubes is presented in Figure 3a. The TEM image shows that, a highly ordered crystalline structure of CNT is observed. The clear fringes of graphitic sheets are well separated by 0.34 nm and aligned with a tilted angle of about 2° toward the tube axis. The TEM images of CNTs doped with Fe_2O_3 nanoparticles were also taken in order to verify the presence of nanoparticle ions on the surfaces of the CNTs (as shown in Figure 3 b and c). The distribution and agglomeration of Fe_2O_3 nanoparticles were also investigated. It was observed that, there are formations of white crystal structures of Fe_2O_3 nanoparticles with small sizes and irregular shapes. It can be seen that Fe_2O_3 nanoparticles are spread widely on the surfaces of carbon nanotubes forming very small crystal particles with diameters varying from 1-

5 nm. When the ratio is increased to 30% and 50%, the size of Fe_2O_3 nanoparticles is about 50 nm and agglomerate intensively as indicated in Figure 3d and Figure 3e, respectively.

The doping of Fe_2O_3 nanoparticles on the surfaces of CNTs was also confirmed by energy dispersive X-ray spectroscopy (EDX) and XRD diffraction.

The EDX analysis of the undoped and doped CNTs, which represents the atomic weight percentage (%) of the elements such as Fe, O and C, are shown in Table 2. The Fe/C ratios extracted from the EDX are close to the calculated values of the prepared samples.

Figure 4 shows the X-ray diffraction patterns of undoped and doped CNTs and pure α-Fe_2O_3. It has been observed that, the XRD diffraction pattern of pure α-Fe_2O_3 is similar to doped Fe_2O_3 nanoparticles confirming the presence of α-Fe_2O_3 crystal nanoparticles on the surfaces of CNTs. There is one characteristic peak of CNTs which was observed at 2θ of 27, while other characteristic peaks were found at 2θ, 34.36, 42, 50, 54, 63, 65, 72 and 75 which corresponds to α-Fe_2O_3. These results revealed that, the α-Fe_2O_3 particles were successfully attached to the CNTs.

The thermal oxidation and degradation of the materials is an important factor as it determines the upper temperature limit. Figure 5 depicts the TGA results of undoped and doped carbon nanotubes. The results showed that, the initial oxidation temperature of undoped CNTs under air condition starts approximately at 580°C and then reaches a complete oxidation at 670 °C. While the initial and final oxidation temperatures of doped CNTs with 1, 10, 30 and 50 wt. % reduces to 520, 480, 460, 450 and 620, 600, 550, 500 °C respectively as shown in Figure 5. It has been noticed that, the loading of Fe_2O_3 nanoparticles doped on CNTs acted as a heating accelerator agent, which accelerated the heat transfer to the body of the CNTs as can be seen by the faster

combustion of the doped CNTs (oxidization) compared to undoped CNTs. In addition to the measurement of the thermal stability of CNTs, the TGA provides an accurate estimate of the loading of Fe_2O_3 nanoparticles doped on CNTs by comparing the residues for the complete oxidation of doped and undoped CNTs. The final remaining residues of undoped and doped CNTs with 1, 10, 30 and 50 wt. % Fe_2O_3, are 0.99, 2.05, and 8.8, 32 and 48 wt. %, respectively.

The BET surface area analysis was conducted to measure the surface area of undoped and doped CNTs. The analysis was performed using a Micromeritics (ASAP 2020) instrument and the interpretation of the results was based on the adsorption-desorption of liquid N_2 at 77 K. The BET surface area values obtained for the undoped and doped CNTs with 1, 10, 30, and 50 wt% Fe_2O_3 nanoparticles were 137.7, 226.6, 295.4, 128, 74.86 m^2/g respectively, as shown in Figure 6. Figure 6 shows that the surface area is enhanced for the iron oxide nanoparticles with 1 and 10 wt% nanoparticles doped on the surface of the CNTs and hence the number of sites for adsorption is increased. On the other hand, when the doping level increased to 30 and 50 wt% the surface area of CNTs decreased due to the aggregation and agglomeration of iron nanoparticles thus forming a large cluster of nanoparticles that blocks some of the available pore surfaces on the CNTs.

The loading of Fe_2O_3 nanoparticles on the negative surfaces of carbon nanotubes has a great impact on the stability of the oil emulsion breaking process, which substantially improves the oil adsorption capacity on the surface of the carbon nanotubes. The existence of the Fe^{3+} on the surfaces of carbon nanotubes will modify the liquid/liquid and liquid/air surface properties. For instance, Fe^{3+} serves to decrease the interfacial tension between the dispersed oil phase and the water and then increases the interfacial tension between the air bubbler and the oil phase. Accordingly, loading Fe_2O_3 nanoparticles on the surface of carbon nanotubes will increase oil

droplet coalescence and enhancing this coalescence should also enhance the oil adsorption uptake. This phenomenon can be explained through the zeta potential measurements.

The surface charge density of undoped and doped CNTs was studied using a Zeta Seizer Analyzer. Table 3 shows that the undoped carbon nanotubes have a negative charge of -42.6mV in the oil-in-water emulsion. Loading Fe_2O_3 nanoparticles on the negative surface of carbon nanotubes decreases the negative sign of the zeta potential by overcoming the repulsive effects of the electrical double layers to allow the finely sized oil droplets to form larger droplets through coalescence. In this study, the zeta potential of oil droplets was not measured. However, literature indicates that oil droplets have a large negative zeta potential typically ranging between -35 mV to -25 mV [28, 29]. This implies that electrostatic repulsion would make an attachment between oil droplets highly unlikely [30, 31]. Thus, it is important to decrease the electrostatic repulsion barrier in oil emulsion systems to further improve the adsorption process. It is observed that increasing the percentage of Fe_2O_3 loaded on the negative surface of carbon nanotubes reduces the magnitude of the zeta potential of oil droplets and this appears to be a crucial factor in the adsorption performance of such emulsion systems. This finding is in good agreement with adsorption measurements in this work, as the percentage of the α–Fe_2O_3 on the surface of carbon nanotubes increased the removal of the emulsified oil from the water. It is also worthy to mention that the similarities in the adsorption capacity for 30 wt.% and 50 wt.% of α–Fe_2O_3 loaded on the surface of carbon is a result of the similarity in the zeta potential values.

3.2. Effect of contact time

In order to find the optimum equilibrium and contact time for maximum uptake of emulsified oil from water by undoped and doped CNTs, experiments were performed at different contact times

ranging from 0 to 2 h. All the other parameters including shaking speed, adsorbent dosage, initial concentration and pH were kept constant at 400 rpm, 20 mg, 841 mg/L and pH 7 respectively. The samples were taken at different preset time intervals and the concentration of remaining oil was measured using a TOC analyzer. The dynamic sorption of oil with both undoped and doped CNTs with different concentrations of iron oxide nanoparticles is shown in Figure 7.

Oil removal from produced water with both undoped and doped CNTs increases with the increase in contact time and reaches a maximum adsorption capacity after 20 minutes. The presence of iron nanoparticles doped CNTs enhances the removal efficiency and adsorption capacity compared to undoped CNTs. The maximum removal efficiency of undoped and doped CNTs with 1, 10, 30, and 50 wt. % of Fe_2O_3 nanoparticles were 87.0, 96.09, 96.37, 96.62, and 98.52% respectively. The amount of sorbent oil on the particles increases rapidly during the initial stage and then progressively reaches 90% equilibrium capacity in 10-15 minutes adsorption time. The high removal rate at the beginning of the contact time was due to the large number of vacant binding sites available for the adsorption of oil. This rapid uptake coupled with a high sorption capacity are two of the most significant properties for an oil to be sorbed by CNT. As the outside surface of CNTs becomes exhausted and saturated with oil droplets, the rate of oil uptake starts to decrease and reaches equilibrium. The doped CNTs reach equilibrium faster than undoped CNTs by almost a factor of two. Wang et. al [21] used magnetic CNT and they found that the equilibrium reached maximum adsorption after 90 min contact time which is 3 times larger than the time needed to reach equilibrium in this study.

3.3. Effect of adsorbent dosage

Batch adsorption experiments with different adsorbent masses ranging from 5 mg to 35 mg have been designed to investigate the effect of adsorbent dosage on removal efficiency of oil from

water using undoped and doped CNTs. For this series of experiments all the experimental parameters, except adsorbent mass, including agitation speed, initial oil concentration and contact time were kept constant at 400 rpm, 841 mg/L and 2h. Figure 8 shows the final oil concentration decreases with increasing adsorbent dosage. The maximum oil removal percentages of oil using undoped and doped CNTs were obtained at adsorbent masses of 30 mg and 25 mg respectively. It was noticed that, the percentage oil removal for all Fe_2O_3 nanoparticles loadings was similar at high CNTs dosages, however, at low adsorbent doses, the oil removals were more sensitive to the Fe_2O_3 nanoparticles loadings. The higher removal percentage by doped CNTs is due to the larger available active adsorption sites and increased oil droplet coalescence.

3.4.Adsorption isotherms for oil removal

The equilibrium adsorption capacity is important in the design of adsorption systems. Equilibrium studies in adsorption indicate the potential maximum capacity of the adsorbent during the treatment process. The effect of initial concentration on oil adsorption was investigated by varying the initial concentration of oil (from 400 mg/L up to 7500 mg/L) at optimum fixed experimental conditions (adsorbent dosage: 20 mg and contact time: 2h). Equilibrium adsorption data were used to determine the maximum adsorption capacity of the undoped and doped CNTs. The Langmuir, Freundlich, and Temkin isotherm models were employed to demonstrate the adsorption data.

The Langmuir, Freundlich, and Temkin equations were used to describe the data derived from the adsorption of oil by the different adsorbents over the entire parameters range studied. Based on Figures 9 and 10, the adsorption capacities (Q_e) and adsorption intensities were determined from the slope and the intercept of each equilibrium graph, respectively. By comparing the Langmuir

and Freundlich isotherms data in Table 4, the Freundlich isotherm gives a better fit with higher correlation coefficients for both undoped and doped CNTs.

Based on the data analysis, the adsorption data cannot be described by Langmuir isotherm the coefficients of determination (R^2) are less than 0.5 for all samples. On the other hand, both undoped and doped CNTs show a very good agreement with the Freundlich model. The Langmuir isotherm assumes monolayer coverage on a homogeneous surface with identical adsorption sites and implying single component adsorption with a constant energy of adsorption. For adsorption of oil on CNT sample with many different hydrocarbon compounds, Langmuir type adsorption is not expected as the system is much more dynamic due to the hydration forces, mass transport effects etc.. On the other hand, the adsorption data for undoped and doped CNTs are well described by the Freundlich isotherm. The Freundlich isotherm is commonly used to describe the adsorption characteristics for heterogeneous surfaces and systems where it is easier to handle mathematically in more complex calculations (e.g. modeling the dynamic column behavior). Therefore, the Freundlich isotherm model was employed to describe the adsorption of oil (and its myriad of hydrocarbon compounds) on the surface of all the adsorbents. The Freundlich isotherm describes an adsorption process which is not restricted to the formation of a monolayer and oil multilayering occurs. Therefore, the amount of oil adsorbed on CNT is the summation of adsorption on all sites, with the stronger energy binding sites being occupied initially, until the adsorption energies exponentially decreased upon the completion of the adsorption process. Furthermore, it can also account for multilayer coverage, which is important in the present study.

The Temkin isotherm model analysis results are shown in Figure 10 and Table 5. The constants in the Temkin isotherm are found by plotting Q_e versus ln C_e. The correlation coefficients are between 0.8 and 0.9 for the different adsorbents. The A value which is an indication of binding energy shows that there is a linear increase in the standard enthalpy of adsorption with surface coverage and when the surfaces of CNTs doped by Fe_2O_3 nanoparticles, surface binding energy increases. This can be related to the zeta potential and the increase in charge density by introducing Fe_2O_3 nanoparticles.

3.5. Adsorption kinetics for the removal of oil

The modeling of the kinetics for oil adsorption on CNTs was investigated using three widely used sorption models, namely, the Lagergren pseudo-first order, pseudo-second-order and intraparticle diffusion model. Linearized plots of the three models are shown in Figures 11, 12 and 13 and the parameters of the second order equations are tabulated in Table 6.

From Figure 11, it can be seen that the data do not fit very well to the first order model, as the R^2 values are less than 0.8 in most cases. The data in Table 5 show that, the value of the rate constant k_2 is lowest for undoped CNTs and increases as the iron dosage into the CNTs increases. The equilibrium adsorption capacity of undoped CNTs is lower than that doped CNTs too, due to the availability of more active adsorption sites and increasing surface charge density (Figure 12). The results also imply that different percentage loadings of iron on CNT do not have a major impact on the equilibrium capacity of the CNTs.

Figure 13 shows the plot of Q_t versus $t^{1/2}$ for the intraparticle diffusion model and it is clearly observed that, the plot does not show a linear trend over the entire time range. There are two almost linear regions, but the sorption time of 20 minutes for the oil uptake in the present study

is far too short for an intraparticle diffusion mechanism. Nevertheless, the $t^{1/2}$ plot does give some visible insight to the mechanism by showing two time regions. The primary linear part might be explained as external surface adsorption, in which the oil particles diffuse through the solution to the external surface of the adsorbent. The second and intermediate linear portion refers to a slower adsorption into the pores of the adsorbent with a slower rate than the first portion. During the first few minutes, layers of oil build up on the external surface of the CNTs; a strongly bound layer of oil due to adhesion and then looser bound layers due to cohesion. This represents most of the oil sorption capacity. After several minutes a slower diffusion of oil into the pores occurs representing about 5-10% of the capacity. Table 7 summarizes the external mass transfer rate parameter (k_i) for all five adsorbents found from the linear fitting analyses of the data. The fits are for the values of the intercept C offer information regarding the thickness of the boundary layer.

In comparison to other carbon nanomaterials, the materials in this study showed better performance. For example, magnetic CNT developed by Wang et al. [21] showed maximum adsorption capacity of 6.6 g/g while our materials have maximum capacity of 7.7 g/g regardless of their more complex preparation method that could be costly to scale up. Also, vertically aligned CNT (VACNT) developed by Liu et al. [22] achieved sorption capacity (12 g/g) slightly higher than our materials' capacity. The advantage of our bulk and random CNT material is their lower cost compared to VACNT. On the other hand, CNT sponge [14][17] has an order of magnitude higher adsorption capacity when used for cleanup of oil spill from the surface of water but it was not tested for separation of oil from oil-water emulsion. Hybrid materials such as CNT-graphene aerogel [11][23] also have been used in literature for oil removal with comparable adsorption capacity to that used in this study. The unique property of CNT-Fe_2O_3

composite studied here is its fast rate of reaction in comparison to other material in literature for application of oil removal. Fast rate of reaction can reduce retention time when designing the adsorption column which can save time and economically more feasible."

3.6.CNT removal from water

Figure 14 provides a qualitative assessment of the performance of CNT in oil-water adsorption. Figure 14a shows the gasoline-water emulsion prepared by sonication without surfactants, as the water-oil interface is clearly visible due to the light-scattering property of oil droplets. Figure 14b shows the CNTs in water as settle to the bottom of the tube due to the lack of adsorption and hydrophobic nature of the CNTs. After addition of CNTs to the solution, the CNTs are freely dispersed in the gasoline-water emulsion by CNTs aggregation around the oil droplets (Fig. 14c). To compare the behavior with CNTs in water only without oil, Figure 14c is taken and most of the CNTs are undispersed and settle at the bottom of the tube. After 2 hours of the adsorption process (Figure 14d) most of the CNTs particulates float on the top of the tube due to the coverage by oil droplets. After 6 hours (Figure 14e) the CNT adsorbs more oil and there is less CNT observed in the tube and most of them are floating on the surface. Figure 14f shows full removal of oil by CNTs as the water is clear after 24 h with all CNTs at the top of the tube. The floating CNTs were removed from the clean water by a conventional sand filtration by placing a sand layer in a sand filtration column (Figure 14g). The effluent of the sand bed is clear water with no evidence of CNT particles. This demonstration provides support for a feasibility study to create an industrial treatment process consisting of the CNTs-oil adsorption process, sedimentation, and sand filtration to fully remove oil and CNT from water and recycle fresh water.

To remove CNT from the oil/water emulsion after treatment, ethanol was used to extract the oil from CNTs. The remaining residue is agglomerated CNTs that can be used again for oil removal. In order to develop an engineering treatment design process several parameters should be taken into account to enhance this cost-effective engineering separation technique. First, the reusability and regeneration of modified CNTs with iron oxide should be considered [32, 33]. Second, the presence of different co-adsorbates and ions in the aqueous solution along with oil should be examined. Influence of constituents such as other hydrocarbons, heavy metal ions, and particulate matter in the emulsion may create adsorption competition and affect the removal efficiency. For an industrial scale process, wastewater does not contain only one constituent and usually is a mixture of several compounds. The presence of such materials may interact with the crystallinity of the CNTs and consequently change the physicochemical properties of modified CNT and ultimately their interaction with oil droplets. Finally, advancements in material synthesis, application and reuse can help improving the economic competitiveness of the treatment process by modified CNT. Consequently, the first stage is the selection of appropriate CNT material which has been carefully done throughout this study.

4. Conclusion

Modified carbon nanotubes by iron nanoparticles have been synthesized in this study by employing the exclusive physicochemical properties of carbon nanotubes. The modified

carbon nanotubes have proved to be very promising for separating oil particles from water. The present study shows the removal efficiency and adsorption of gasoline oil in aqueous solution using modified carbon nanotubes with iron oxide nanoparticles (Fe_2O_3) prepared using the wet impregnation method. The equilibrium data were fitted to the Langmuir, Temkin and Freundlich isotherm models, with the Freundlich isotherm providing the best correlation of the experimental data. The kinetics of the process were studied using three different models (psedou-first order, psedou-second order, and intraparticle diffusion models) and it was observed that the oil adsorption was correlated best with the pseudo-second-order sorption kinetics model. Visual interpretation of the intraparticle diffusion model revealed that the process is not diffusion controlled and the diffusivity of oil on to the CNT surface can be divided into two global processes, namely, an external surface film phase and a pore filling phase. The short time to reach 90% equilibrium capacity, of 15-20 minutes, and the low R^2 values indicates the oil uptake is not controlled by intraparticle diffusion. The results also indicate that oil strongly adsorbed to the surfaces of these adsorbents suggesting that these forms of carbon based adsorbents have great potential to be good adsorbents and can be applied for the removal of oil in water treatment. This study propose separating the CNT from treated water using sand filtration as a standard means of filtration used by industries is feasible.

Acknowledgment

The authors are grateful to the Qatar Environment and Energy Research Institute (QEERI), Qatar Foundation for financial support under project WGC-4004. Also, the authors are

grateful to Mr. Faraj Ahmed Abuilliw, General Science and Studies Unit, Hafr AlBatin Community College, Hafr AlBatin, King Fahad University of Petroleum & Minerals (KUFPM), Saudi Arabia for providing raw material for this study.

References

[1] M. Abdullah, A.U. Rahmah, Z. Man, Physicochemical and sorption characteristics of Malaysian Ceiba pentandra (L.) Gaertn. as a natural oil sorbent, Journal of hazardous materials 177 (2010) 683-691.

[2] Z. Khatib, P. Verbeek, Water to value-produced water management for sustainable field development of mature and green fields, SPE International Conference on Health Safety and Environment in Oil and Gas Exploration and Production, Society of Petroleum Engineers, 2002.

[3] J.A. Veil, M.G. Puder, D. Elcock, R.J. Redweik Jr, A white paper describing produced water from production of crude oil, natural gas, and coal bed methane, Argonne National Laboratory, Technical Report (2004).

[4] U. EPA, US EPA.

[5] M. Santander, R. Rodrigues, J. Rubio, Modified jet flotation in oil (petroleum) emulsion/water separations, Colloids and Surfaces A: Physicochemical and Engineering Aspects 375 (2011) 237-244.

[6] S. Sabir, Approach of cost-effective adsorbents for oil removal from oily water, Critical Reviews in Environmental Science and Technology (2014) 00-00.

[7] D.D. Nguyen, N.-H. Tai, S.-B. Lee, W.-S. Kuo, Superhydrophobic and superoleophilic properties of graphene-based sponges fabricated using a facile dip coating method, Energy & Environmental Science 5 (2012) 7908-7912.

[8] Y. Nishi, N. Iwashita, Y. Sawada, M. Inagaki, Sorption kinetics of heavy oil into porous carbons, Water Research 36 (2002) 5029-5036.

[9] X. Zhang, L. Chen, T. Yuan, H. Huang, Z. Sui, R. Du, X. Li, Y. Lu, Q. Li, Dendrimer-linked, renewable and magnetic carbon nanotube aerogels, Materials Horizons 1 (2014) 232-236.

[10] Y. Zhao, C. Hu, Y. Hu, H. Cheng, G. Shi, L. Qu, A Versatile, Ultralight, Nitrogen-Doped Graphene Framework, Angewandte Chemie 124 (2012) 11533-11537.

[11] X. Dong, J. Chen, Y. Ma, J. Wang, M.B. Chan-Park, X. Liu, L. Wang, W. Huang, P. Chen, Superhydrophobic and superoleophilic hybrid foam of graphene and carbon nanotube for selective removal of oils or organic solvents from the surface of water, Chemical Communications 48 (2012) 10660-10662.

[12] R. Evershed, R. Berstan, F. Grew, M. Copley, A. Charmant, E. Barham, H. Mottram, G. Brown, Water-repellent legs of water striders, Carbohyd. Res 113 (1983) 291-299.

[13] L. Ci, S.M. Manikoth, X. Li, R. Vajtai, P.M. Ajayan, Ultrathick freestanding aligned carbon nanotube films, Advanced Materials 19 (2007) 3300-3303.

[14] X. Gui, J. Wei, K. Wang, A. Cao, H. Zhu, Y. Jia, Q. Shu, D. Wu, Carbon nanotube sponges, Advanced Materials 22 (2010) 617-621.

[15] Ihsanullah, F.A. Al-Khaldi, B. Abu-Sharkh, A.M. Abulkibash, M.I. Qureshi, T. Laoui, M.A. Atieh, Effect of acid modification on adsorption of hexavalent chromium (Cr(VI)) from aqueous solution by activated carbon and carbon nanotubes, Desalination and Water Treatment (2015) 1-13.

[16] V.K. Upadhyayula, S. Deng, M.C. Mitchell, G.B. Smith, Application of carbon nanotube technology for removal of contaminants in drinking water: a review, Science of the total environment 408 (2009) 1-13.

[17] X. Gui, H. Li, K. Wang, J. Wei, Y. Jia, Z. Li, L. Fan, A. Cao, H. Zhu, D. Wu, Recyclable carbon nanotube sponges for oil absorption, Acta Materialia 59 (2011) 4798-4804.

[18] X. Gui, Z. Zeng, Z. Lin, Q. Gan, R. Xiang, Y. Zhu, A. Cao, Z. Tang, Magnetic and highly recyclable macroporous carbon nanotubes for spilled oil sorption and separation, ACS applied materials & interfaces 5 (2013) 5845-5850.

[19] M.-Q. Zhao, J.-Q. Huang, Q. Zhang, W.-L. Luo, F. Wei, Improvement of oil adsorption performance by a sponge-like natural vermiculite-carbon nanotube hybrid, Applied Clay Science 53 (2011) 1-7.

[20] Z. Fan, J. Yan, G. Ning, T. Wei, W. Qian, S. Zhang, C. Zheng, Q. Zhang, F. Wei, Oil sorption and recovery by using vertically aligned carbon nanotubes, Carbon 48 (2010) 4197-4200.

[21] H. Wang, K.-Y. Lin, B. Jing, G. Krylova, G.E. Sigmon, P. McGinn, Y. Zhu, C. Na, Removal of oil droplets from contaminated water using magnetic carbon nanotubes, Water Research 47 (2013) 4198-4205.

[22] T. Liu, S. Chen, H. Liu, Oil Adsorption and Reuse Performance of Multi-Walled Carbon Nanotubes, Procedia Engineering 102 (2015) 1896-1902.

[23] H. Hu, Z. Zhao, Y. Gogotsi, J. Qiu, Compressible Carbon Nanotube–Graphene Hybrid Aerogels with Superhydrophobicity and Superoleophilicity for Oil Sorption, Environmental Science & Technology Letters 1 (2014) 214-220.

[24] H. Yuh-Shan, Citation review of Lagergren kinetic rate equation on adsorption reactions, Scientometrics 59 (2004) 171-177.

[25] Y.-S. Ho, G. McKay, Pseudo-second order model for sorption processes, Process biochemistry 34 (1999) 451-465.

[26] W.J. Weber, J.C. Morris, Kinetics of Adsorption on Carbon from Solution, Journal of the Sanitary Engineering Division 89 (1963) 31-60.

[27] A. Dada, A. Olalekan, A. Olatunya, O. Dada, Langmuir, freundlich, temkin and dubinin–radushkevich isotherms studies of equilibrium sorption of Zn2+ unto phosphoric acid modified rice husk, Journal of Applied Chemistry 3 (2012) 38-45.

[28] J. Hempoonsert, B. Tansel, S. Laha, Effect of temperature and pH on droplet aggregation and phase separation characteristics of flocs formed in oil–water emulsions after coagulation, Colloids and Surfaces A: Physicochemical and Engineering Aspects 353 (2010) 37-42.

[29] S.C. Thickett, P.B. Zetterlund, Graphene oxide (GO) nanosheets as oil-in-water emulsion stabilizers: Influence of oil phase polarity, Journal of Colloid And Interface Science 442 (2015) 67-74.

[30] M. Karhu, T. Leiviskä, J. Tanskanen, Enhanced DAF in breaking up oil-in-water emulsions, Separation and Purification Technology 122 (2014) 231-241.

[31] G.J. Rincón, E.J. La Motta, Simultaneous removal of oil and grease, and heavy metals from artificial bilge water using electro-coagulation/flotation, Journal of Environmental Management 144 (2014) 42-50.

[32] K. Balasubramanian, M. Burghard, Chemically functionalized carbon nanotubes, Small 1 (2005) 180-192.

[33] J.-P. Salvetat, J.-M. Bonard, N. Thomson, A. Kulik, L. Forro, W. Benoit, L. Zuppiroli, Mechanical properties of carbon nanotubes, Applied Physics A 69 (1999) 255-260.

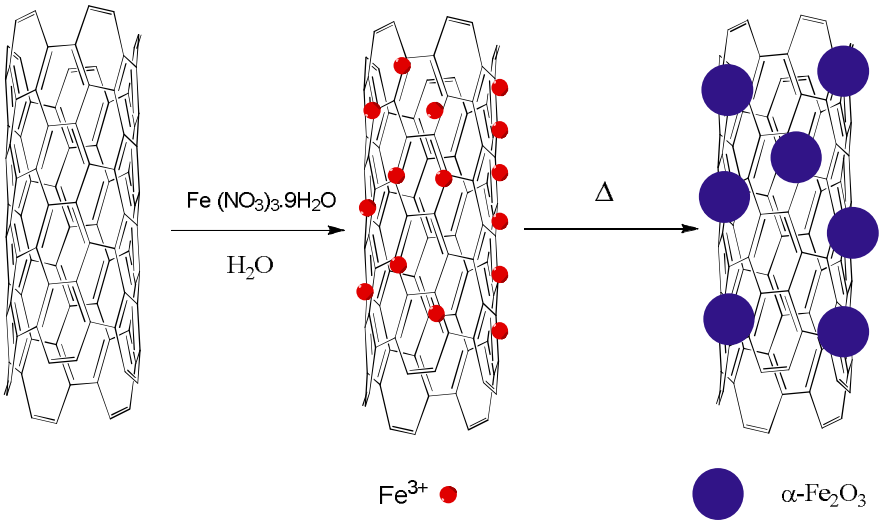

Figure 1: Schematic illustrations of the synthesis processes used to produce hematite nanowires using CNTs as supports

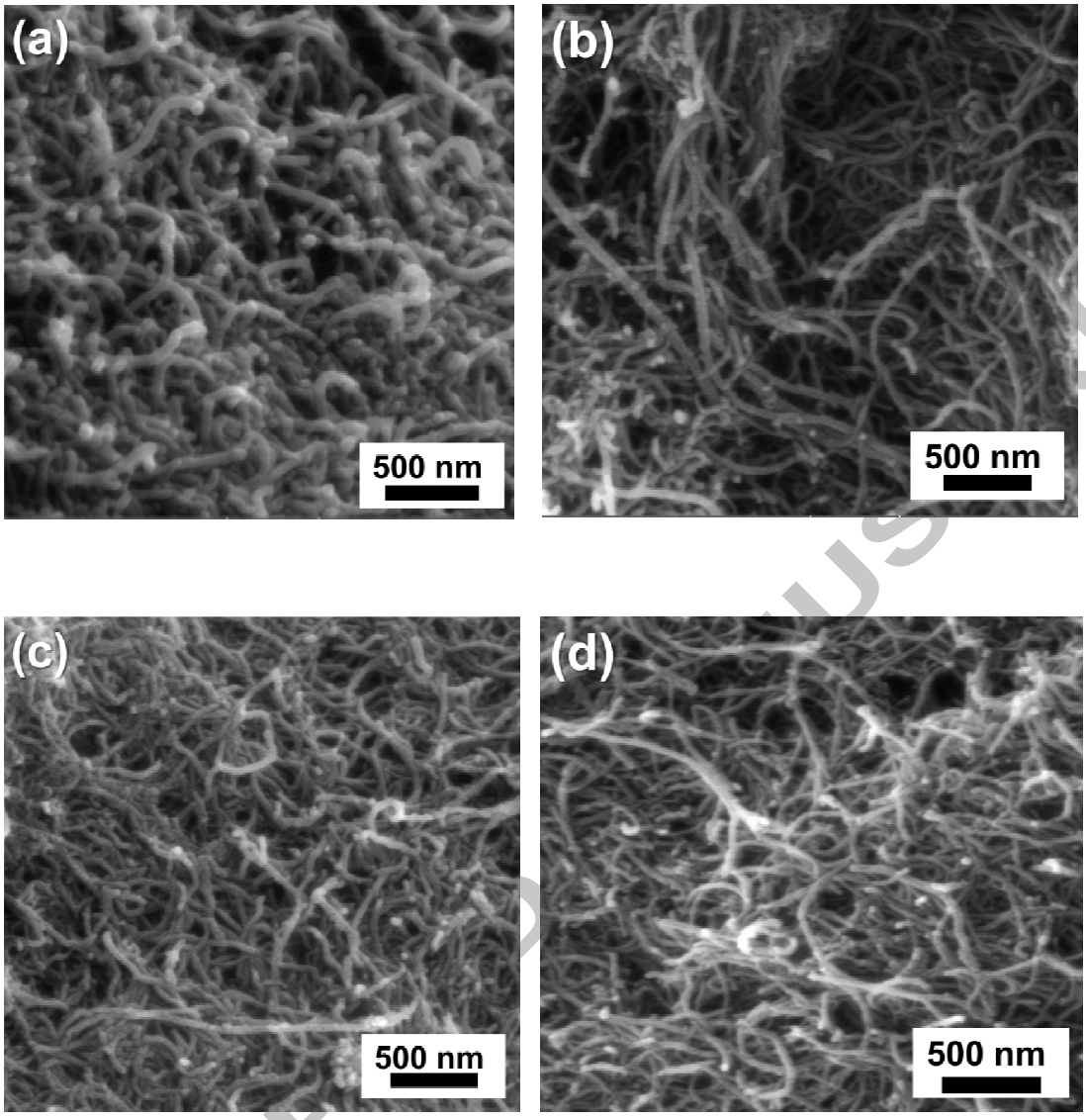

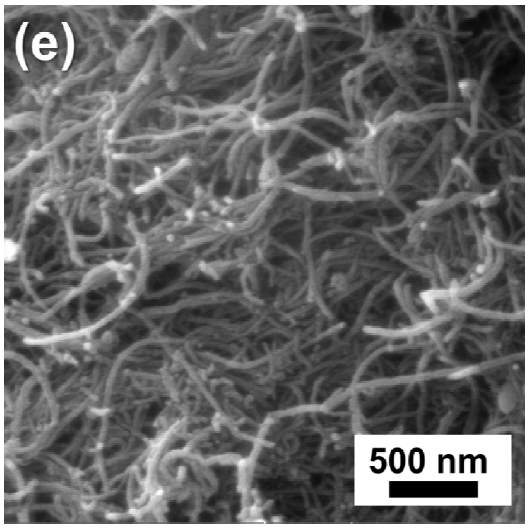

Figure 2: FE-SEM images of undoped CNTs (a) and doped CNT with with 1 % (b), 10 % (c), 30 % (d), and 50% iron oxide nanoparticles

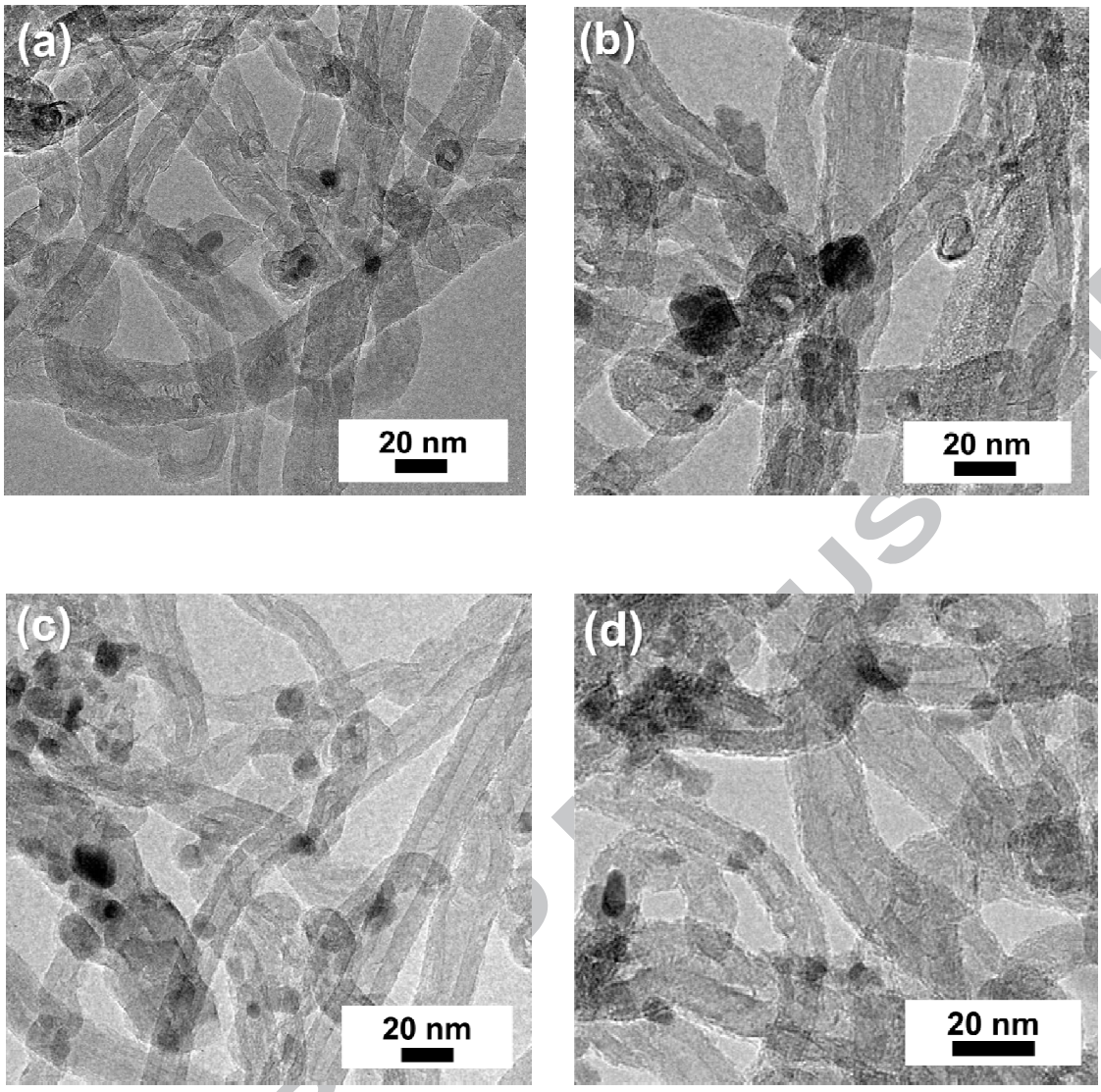

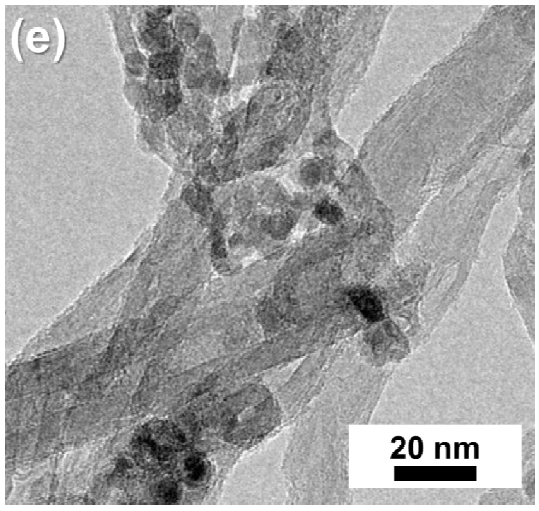

Figure 3: TEM image of pure CNTs (a), and Fe_2O_3 /CNT nano-composites with 1 % (b), 10 % (c), 30 % (d), and 50% Fe_2O_3 content

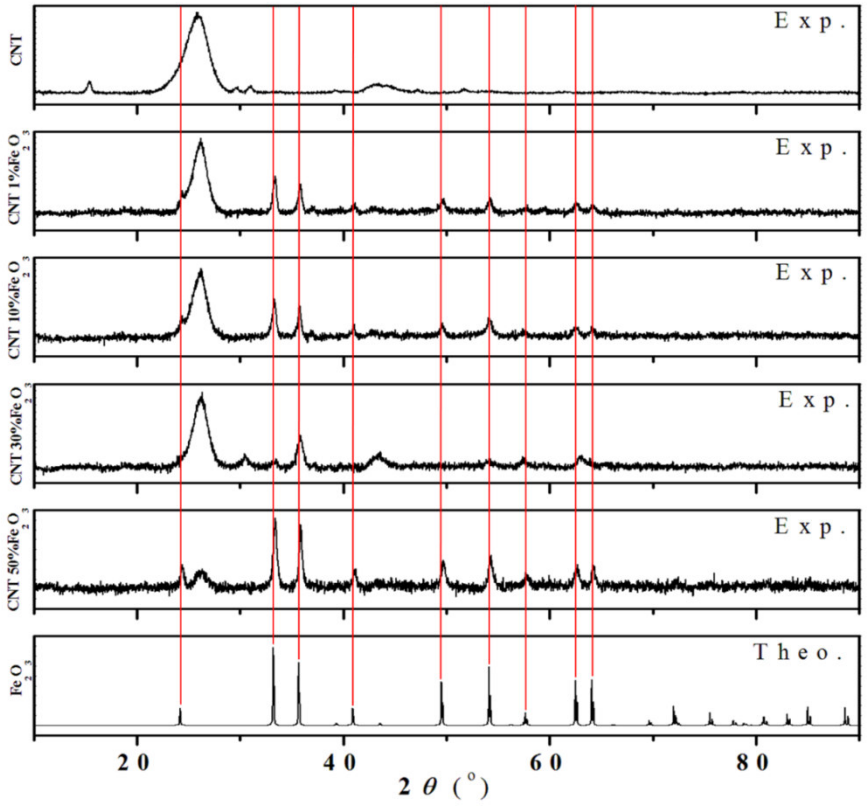

Figure 4: XRD patterns of the α-Fe_2O_3/CNT composites, α-Fe_2O_3, and Pure CNT

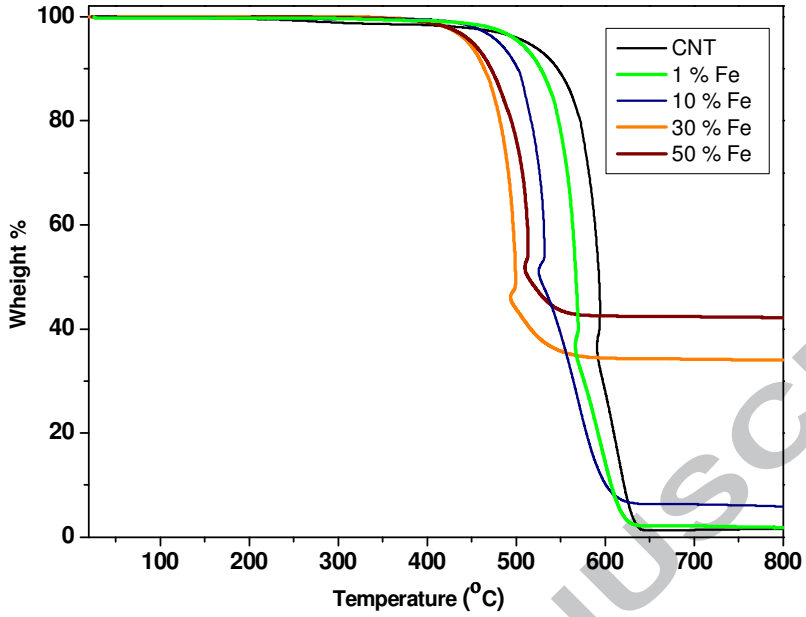

Figure 5: TGA and DTG curves of CNT– α-Fe_2O_3 under O_2 atmosphere at 10 °C /min

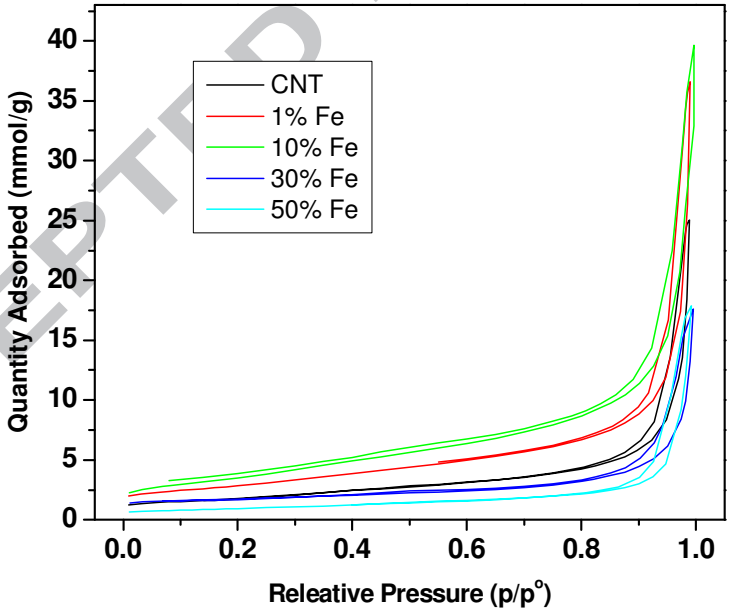

Figure 6: N_2 Adsorption-desorption isotherms of CNT and CNT/ Fe_2O_3 composites

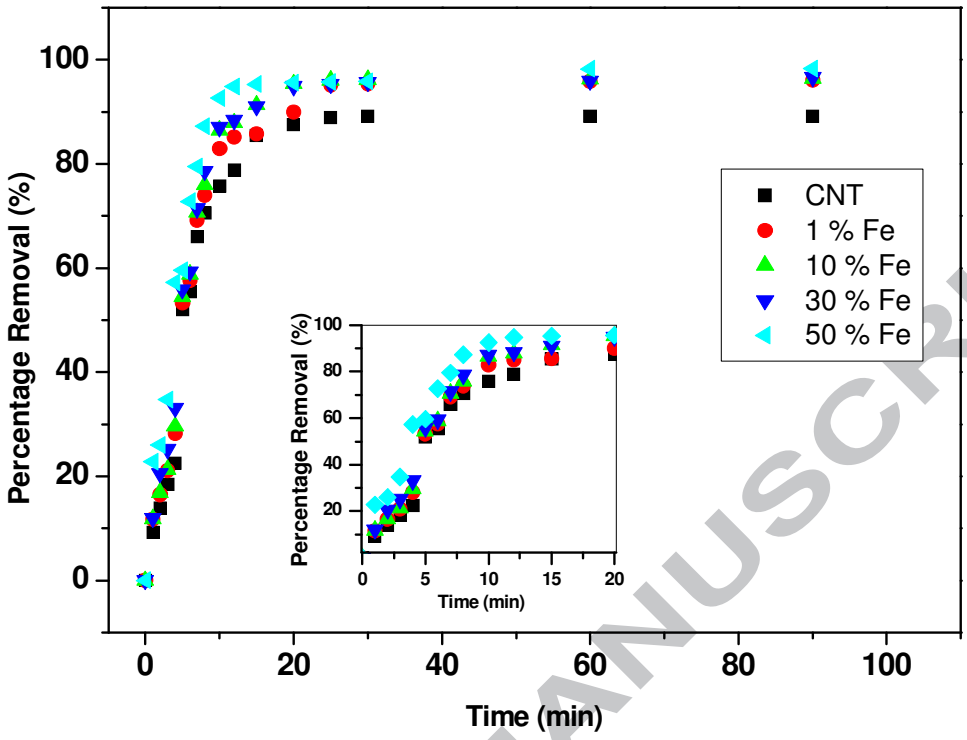

Figure 7: The effect of contact time on the percentage removal of oil

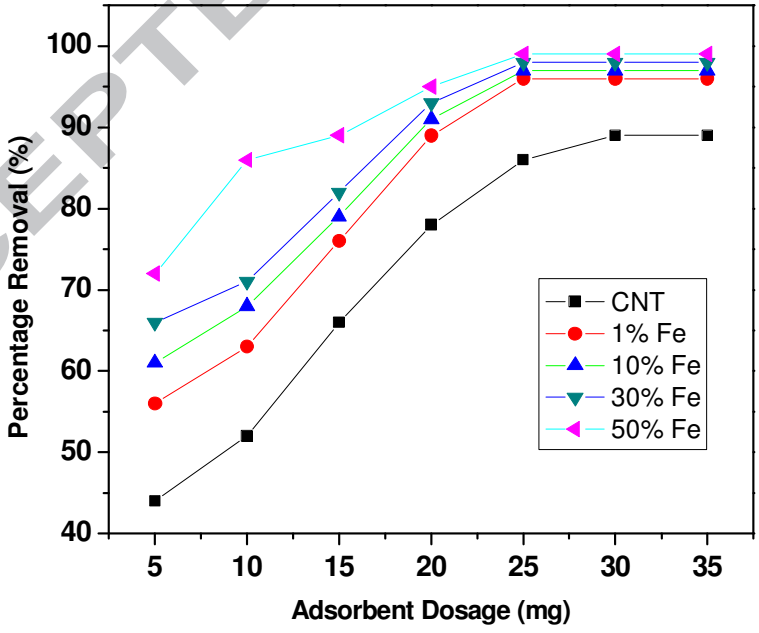

Figure 8: Effect of adsorbent dosage on the percentage removal of oil (oil concentration: 841 mg/L)

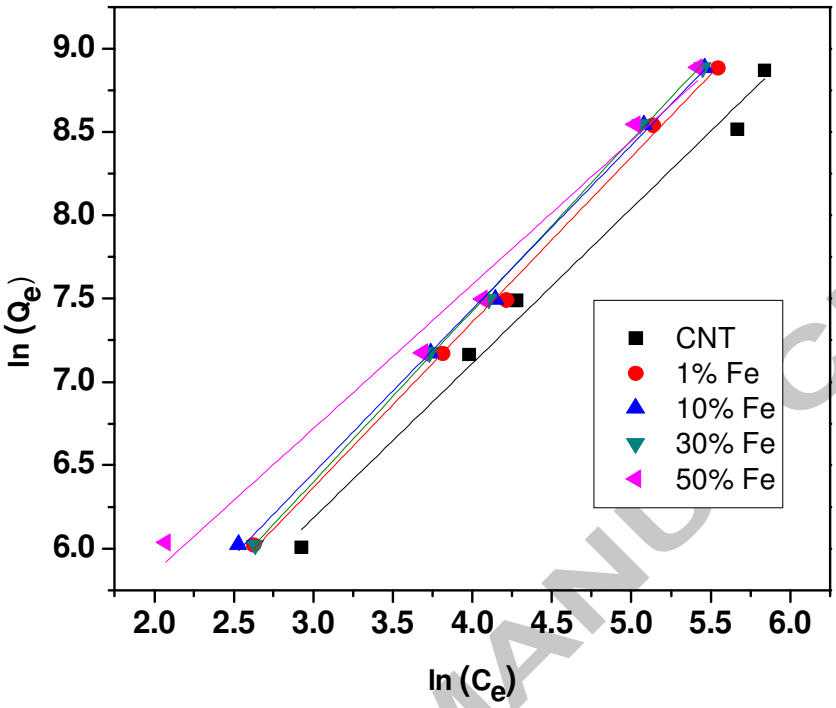

Figure 9: Freundlich adsorption isotherm of oil adsorbed by raw CNT and modified CNTs

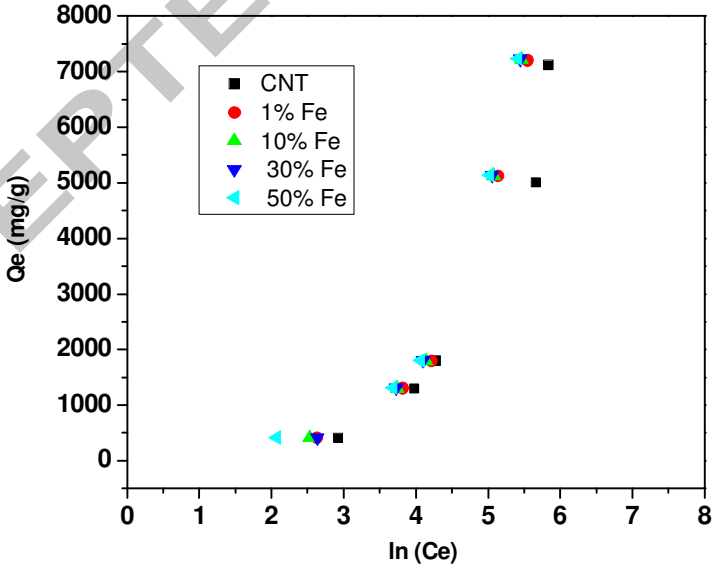

Figure 10: Temkin adsorption isotherm of oil adsorbed by raw CNT and modified CNTs

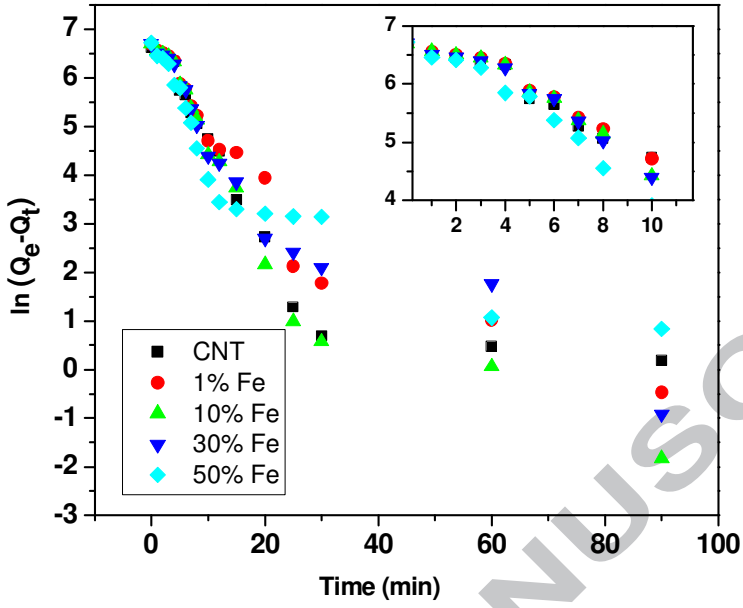

Figure 11: Pseudo-first-order kinetics for the adsorption of oil with undoped and doped (oil concentration: 841 mg/L)

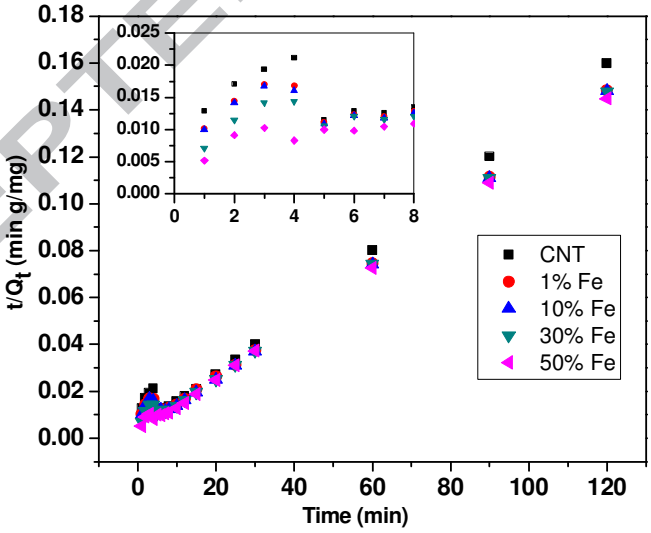

Figure 12: Pseudo-second-order kinetics for the adsorption of oil with undoped and doped CNTs (oil concentration: 841 mg/L)

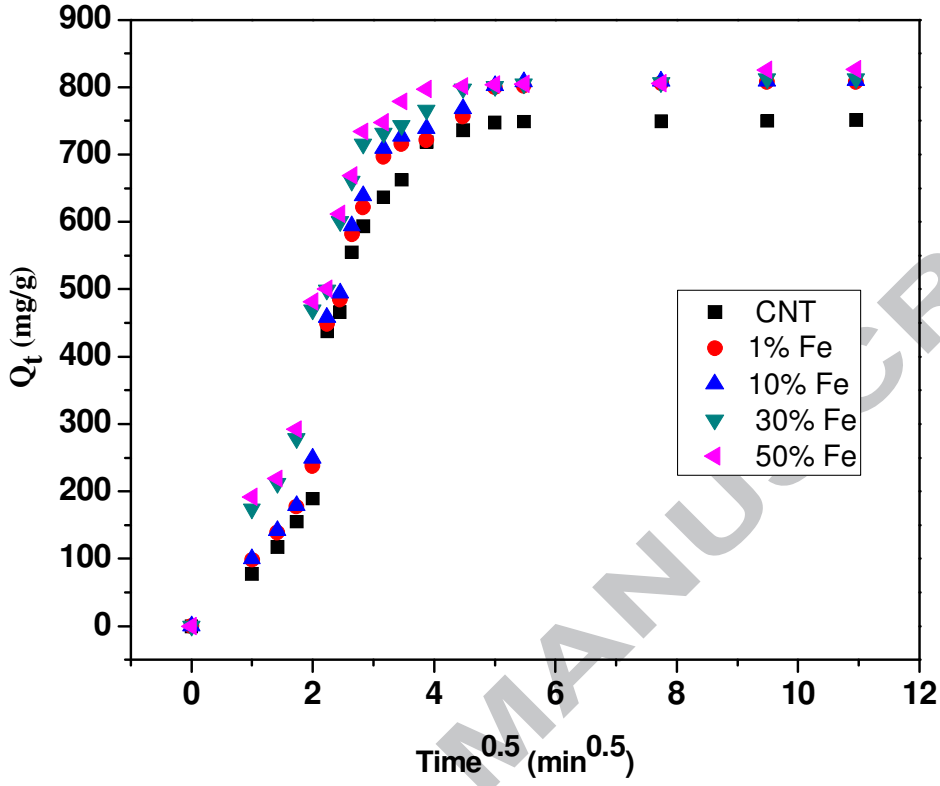

Figure 13: Intraparticle diffusion model for the adsorption of oil with CNT and modified CNT (oil concentration: 841 mg/L)

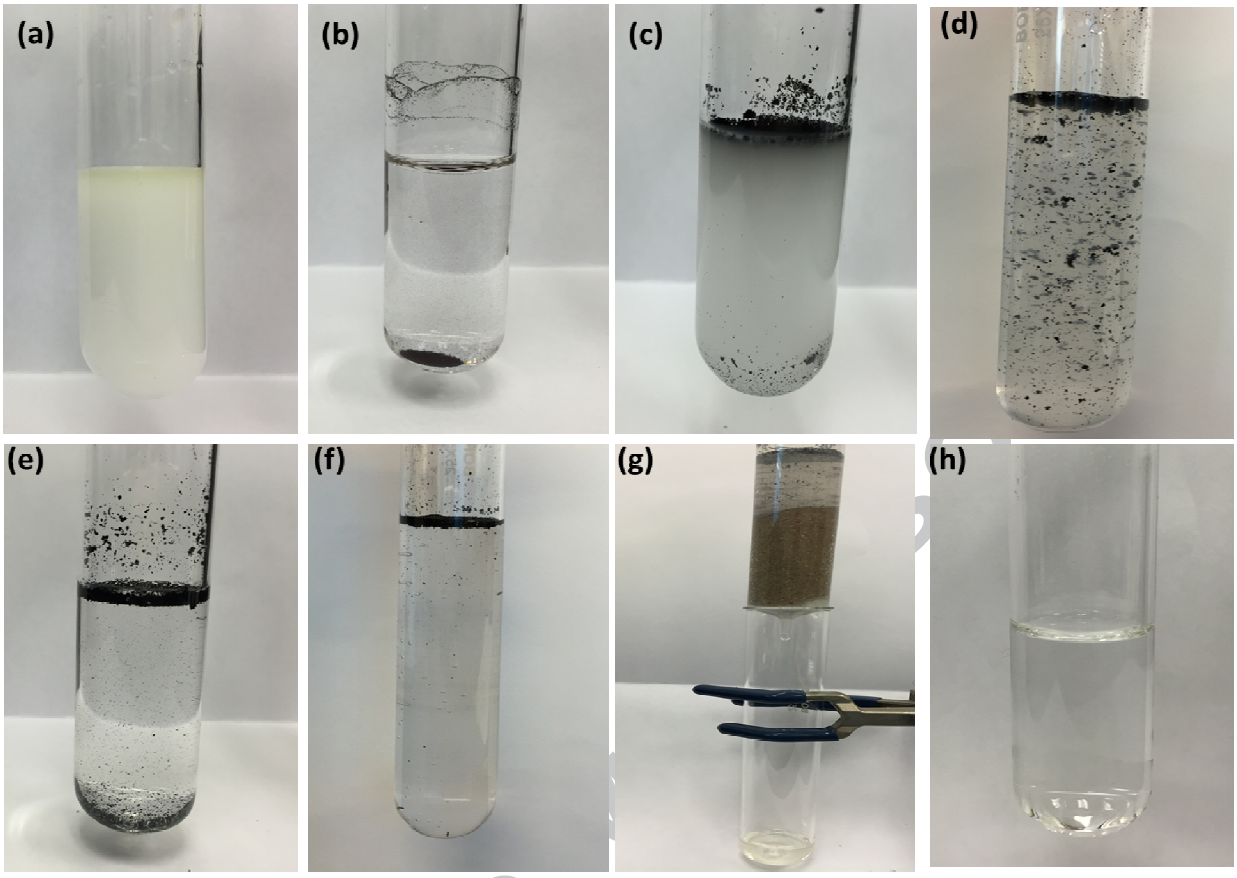

Figure 14: Digital pictures of experimental setup for evaluation of oil-water separation. (a) oil-water emulsion with water-oil interface. (b) CNT in water (no oil). (c) oil-water aqueous solution right after addition of CNT. (d) CNT in water after 2 hour adsorption process. (e) CNT in water 6 hours after adsorption process. (f) CNT in water 24 hours after adsorption process. (g) sand filtration setup for removal of CNT from water. (h) effluent of sand filtration (oil concentration: 7500 ppm).

Table 1: Previous studies on oil removal with different forms of CNT

Adsorbent	Adsorption capacity (g/g)	Type of oil	Reference
CNT sponge	143	Diesel	[14]
Vertically aligned carbon nanotubes	69	Kerosene oil	[20]
Magnetic carbon nanotubes	6.6	Diesel	[21]
Carbon nanotube sponge	110	Diesel	[17]
Multi-walled carbon nanotubes	12	Gasoline	[22]
Magnetic macroporous carbon nanotubes	56	Diesel	[18]
Graphene and carbon nanotube hybrid	85	Compressor oil	[11]
Carbon nanotube–graphene hybrid aerogels	120	Diesel	[23]

Table 2: EDX analysis of commercial CNT and CNT with different percentage of α-Fe2O3

CNT Sample (theo)	**Raw CNTs**	**CNT-Fe_2O_3 (1%)**	**CNT-Fe_2O_3 (10%)**	**CNT-Fe_2O_3 (30%)**	**CNT-Fe_2O_3 (50%)**
Element	**Weight %**	**Weight %**	**Weight %**	**Weight %**	Weight %
C	98.50	94.47	84.53	45.9	37.66
O	1.50	3.65	4.5	23.53	18.60
Fe	0	1.50 (**1**)	11.03 (**10**)	28.08 (**30**)	43.74 (50)
Total %	**100**	**100**	**100**	**100**	**100**

Table 3: Zeta potential of CNTs and α-Fe_2O_3/CNT nano-composites with 1 %, 10 %, 30 and 50% of α- Fe_2O_3

CNT/α–Fe_2O_3	Zeta Potential (mV)
0%	-42.6
1%	-20.5
10%	-17.1
30%	-8.9
50%	-8.3

Table 4: Parameters of Langmuir and Freundlich adsorption isotherm models for oil removal

Parameters	**Langmuir**			**Freundlich**		
	Q_m(mg/g)	K_L(L/mg)	R^2	n	K_F	R^2
CNTs	3.33E+04	7.22E-04	0.51	1.08	53.15	0.99
CNTs- α–Fe_2O_3 1wt%	2.00E+06	1.43E-05	0.00	1.01	29.78	1.00
CNTs- α–Fe_2O_3 10 wt%	5.00E+05	6.23E-05	0.01	1.02	33.25	1.00
CNTs- α–Fe_2O_3 30 wt%	1.25E+05	2.40E-04	0.33	0.98	27.86	1.00
CNTs- α–Fe_2O_3 50 wt%	3.33E+04	1.17E-03	0.23	1.16	62.30	0.99

Table 5: Parameters of Temkin adsorption isotherm for oil adsorption

Samples	Temkin Isotherm			
	A	**B**	**b**	**R^2**
CNT	4.46E-02	2.20E+03	1.13	0.90
1% Fe	5.48E-02	2.32E+03	1.07	0.87
10% Fe	6.00E-02	2.30E+03	1.08	0.85
30% Fe	5.57E-02	2.43E+03	1.02	0.88
50% Fe	8.69E-02	1.98E+03	1.25	0.80

Table 6: Kinetic parameters for second order models

Samples	Second Order Model		
	Q_e (mg/g)	k_2 (g/mgh)	R^2
CNT	7.7E+02	2.7E-04	0.99
1% Fe	8.3E+02	2.3E-04	0.99
10% Fe	8.3E+02	2.9E-04	0.99
30% Fe	8.3E+02	3.7E-04	0.99
50% Fe	8.3E+02	5.5E-04	0.99

Table 7: Kinetic parameters for intraparticle diffusion models

	1st linear part			2nd linear part		
	k_i	C	R^2	k_i	C	R^2
CNT	224.4	-48.7	0.88	2.62	744.9	0.95
1% Fe	266.4	-201.6	0.92	6.11	796.5	0.93
10% Fe	286.4	-228.0	0.93	5.46	798.0	0.83
30% Fe	283.9	-211.8	0.91	0.92	788.9	0.92
50% Fe	257.8	-71.7	0.92	20.21	779.3	0.81

Highlights

- The performance of CNT/Iron oxide composite is analyzed for oil-water separation.
- Increasing the Fe_2O_3 loading on the CNT increased the removal of oil from water.
- The CNT/Iron oxide nano-composite showed adsorption capacity of more than 7 g/g.
- Removal efficiency of 100% is achieved using CNT/Iron oxide Nano-composite.